Available online at www.sciencedirect.com
SCIENCE DIRECT®
ELSEVIER
Journal of Sound and Vibration 273 (2004) 103–123
JOURNAL OF SOUND AND VIBRATION
www.elsevier.com/locate/jsvi

Mechanism of sound generation by low Mach number flow over a wall cavity

M.S. Howe*

Boston University, College of Engineering, 110 Cummington Street, Boston, MA 02215, USA

Received 1 November 2002; accepted 26 April 2003

Abstract

An analysis is made of the mechanism of sound production by nominally steady low Mach number flow over a rigid shallow wall cavity. At very low Mach numbers the dominant source of sound is the unsteady drag, and the aeroacoustic dipole source accompanying this force. A monopole source dependent on the compression of fluid within the cavity is smaller by a factor of the order of the flow Mach number M. The directivity of the dipole sound peaks in directions upstream and downstream of the cavity, and there is a radiation null in the direction normal to the plane of the wall. However, numerical simulations for M as small as 0.1 have predicted significant radiation in directions normal to the wall. This anomaly is investigated in this paper by means of an acoustic Green's function tailored to cavity geometry that accounts for possible aeroacoustic contributions from both the drag-dipole and from the lowest order cavity resonance. The Green's function is used to show that these sources are correlated and that their strengths are each proportional to the unsteady drag generated by vorticity interacting with the cavity trailing edge. When $M \sim 0.01$, the case in most underwater applications, the monopole strength is always negligible (for a cavity with rigid walls). At low Mach numbers exceeding about 0.05 it is shown that the cavity monopole radiation is $O(M^2) \ll 1$ relative to the dipole at low frequencies. At higher frequencies, near the resonance frequency of the cavity, the monopole and dipole have similar orders of magnitude, and the combination produces a relatively uniform radiation directivity, with substantial energy radiated in directions normal to the wall. Illustrative numerical results are given for a wall cavity subject to 'shear layer mode' excitation by the Rossiter 'feedback' mechanism.

*Tel.: 617-484-0656; fax: 617-757-5869.
E-mail address: mshowe@bu.edu (M.S. Howe).

0022-460X/$ - see front matter © 2003 Elsevier Ltd. All rights reserved.
doi:10.1016/S0022-460X(03)00644-8

1. Introduction

Tonal radiation produced by high Reynolds number mean flow over a rectangular wall cavity was originally attributed to broadband excitation of cavity acoustic resonances by turbulence in the shear layer over the cavity mouth [1]. However, oscillations can also be maintained by a laminar mean flow, and laminar flow resonances are often observed to be more intense [2,3]. Tones generated by shallow cavities whose depth $d < L$ = streamwise cavity length (Fig. 1) generally bear little or no correspondence to cavity modes and are not usually harmonically related, but are more closely analogous to the 'edge' tones excited when a thin jet impinges on a wedge-shaped knife edge, and maintained via a 'feedback' mechanism from the wedge to the jet nozzle.

A cavity tone of frequency f generated by flow of mean stream velocity U is typically found to lie within certain well defined bands of the Strouhal numbers fL/U when plotted against flow Mach number. This is consistent with the 'feedback' scheme proposed by Rossiter [1], involving the periodic formation of discrete vortices just downstream of the leading edge of the cavity, and their subsequent interaction with the trailing edge after convection across the cavity mouth. The impulsive sound generated by this interaction propagates upstream within the cavity and causes the boundary layer to separate just upstream of the leading edge. The travel time of a vortex across the cavity $\sim L/U_c$, where the convection velocity $U_c \approx 0.4U - 0.6U$, and the sound radiates back to the leading edge in time L/c_0, where c_0 is the speed of sound. The returning sound therefore arrives in time to reinforce periodic shedding provided

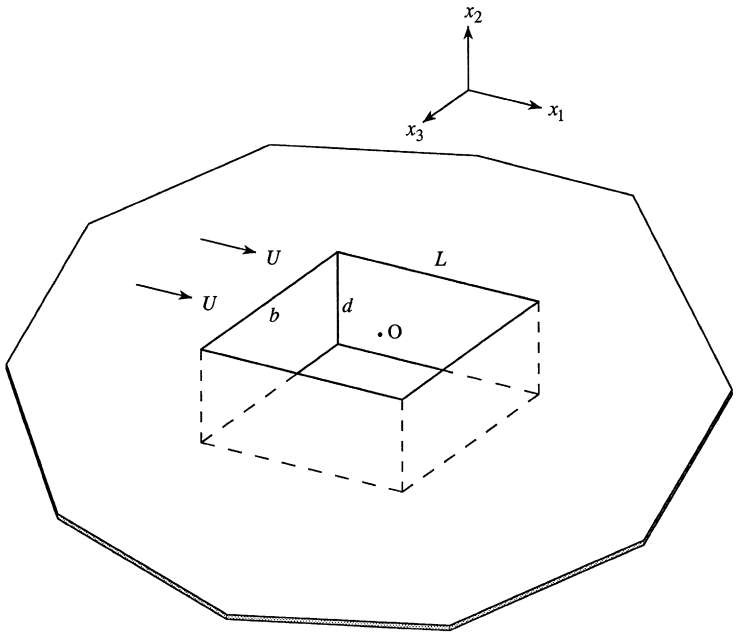

Fig. 1. Schematic configuration of nominally steady, high Reynolds number flow over a rigid, rectangular wall cavity of depth d and streamwise length L.

f satisfies [1]

$$\frac{L}{U_c}+\frac{L}{c_0}\approx\frac{n}{f},\quad n=1,2,\ldots. \tag{1}$$

This formula must be adjusted to obtain detailed agreement with experiment [4–6], by replacing n by $n-\beta$, where β (~ 0.25) determines a 'phase lag' β/f equal to the time delay between (1) the arrival of a vortex at the trailing edge and the emission of the main acoustic pulse, and (2) the arrival of the sound at the leading edge and the release of new vorticity. If account is also taken of the Mach number (i.e. temperature) dependence of the sound speed in the cavity, Rossiter's equation (1) can be written as

$$\frac{fL}{U}=\frac{n-\beta}{\{U/U_c+M/\sqrt{1+(\gamma_0-1)M^2/2}\}},\quad n=1,2,\ldots, \tag{2}$$

where $M=U/c_0$ and γ_0 is the ratio of specific heats of the fluid.

Predictions of the feedback formula (2) for shallow, rectangular cavities with $d/L<1$ agree well with observations at $M>0.2$ for $\beta\approx\frac{1}{4}$ and $U_c/U\approx 0.6$ [6]. The contributions from cavity resonances are important only for deep cavities, and appear to be unimportant unless $d/L>\frac{2}{5}$, when resonances can dominate the radiation provided the Strouhal number also satisfies (2). An extensive discussion of experimental results relating to this and other influences of cavity geometry and mean flow conditions on cavity resonances is given by Ahuja and Mendoza [6] for Mach numbers $M>0.2$. Research prior to 1980 is reviewed by Rockwell [4] and by Rockwell and Naudascher [7], and Grace [8] has summarized recent attempts to simulate numerically cavity noise radiation.

Experiments conducted by Gharib and Roshko [9] in water with a nominally steady impinging mean flow (at $U\sim 1$ m/s) have shown that Rossiter feedback resonances are related to large fluctuations in the drag experienced by the cavity. They identified two hydrodynamic modes of cavity flow oscillations: for 'shorter' cavities relative to the upstream boundary layer thickness (and, according to later work [10], for lower Mach numbers) the unsteady motion over the cavity mouth has the characteristics of an unstable, thin shear layer ('shear layer mode') that generates sound by impingement on the cavity trailing edge, essentially in the manner proposed by Rossiter [1]. Recent numerical studies of two-dimensional cavity flows by Colonius et al. [10] predict strong radiation preferentially in the upstream direction, from a 'source' centred on the cavity trailing edge. Three-dimensional numerical simulations performed by Fuglsang and Cain [11] of the acoustic field *within* a shallow cavity ($L/d=4.5$) at $M=0.85$ also indicated that shear layer instability is the main exciting mechanism, and that it produces a source-like periodic addition and removal of mass near the trailing edge. An analytical, but empirical representation of this edge source had been previously considered by Tam and Block [12]. Flow over longer cavities (or, alternatively, at higher Mach numbers) is characterized by a 'wake mode', involving large scale vorticity ejection from the cavity, producing quasi-periodic separation upstream of the leading edge. The onset of the wake mode is accompanied by a large increase in drag fluctuations. This apparently occurs also at much higher Mach numbers. For example, numerical simulations by Zhang [13] for $L/d=3$ and $M=1.5$, 3 reveal that the violent ejection of vorticity is strongly correlated with sign reversals of the cavity drag coefficient.

The results of the shear layer mode theory of Tam and Block [12] suggested that at very low Mach numbers ($M<0.2$) cavity acoustic resonances must contribute to the radiation, especially for deeper cavities ($L/d<\frac{1}{2}$, say); the 'monopole' nature of such resonances would account for a near omni-directional character of the radiation pattern observed at certain frequencies. They did not pursue this theoretically, although its likely importance had already been anticipated by Plumblee et al. [14] and by East [15]. Similarly, experiments of Yu [16] have confirmed that shallow wall cavities in air at Mach numbers $M\sim0.1$ radiate a substantial amount of radiation directly away from the wall. Numerical and experimental studies at low Mach number by Inagaki et al. [17] have confirmed this conclusion for large cavities with small openings to the mean flow, but shown also how coincidence between the cavity resonance and the Rossiter frequency predicted by (2) resulted in very large amplitude radiation. For shallow cavities trailing edge 'scattering' of shear layer pressure fluctuations appears to be the dominant source, even when feedback is not important. This is in accord with measurements performed by Jacobs et al. [18] for $L/d>7$ and $M<0.4$, for which the radiation peaked in the upstream and downstream directions, although significant radiation in the wall-normal direction was also observed.

According to the theoretical results of Howe [2], the radiation from a shallow cavity at very low Mach number can be ascribed to a dipole source aligned with the mean flow direction whose strength is determined by the unsteady drag. The dipole source strength is strongly coupled to the hydrodynamic motions in and near the cavity, but is essentially the same in character for both the 'shear layer' and 'wake' modes of the cavity oscillations, provided M is sufficiently small. The intensity of the dipole radiation peaks in the upstream and downstream directions, and is null in directions normal to the wall.

This conclusion is apparently incompatible with several of the experiments discussed above and with recent numerical simulations and observations at low Mach numbers. In Hardin and Pope's [19,20] low Mach number scheme, an incompressible representation of the cavity flow is first simulated numerically, and the results are then used to evaluate acoustic 'sources' in a modified system of compressible flow equations. At $M=0.1$ their predictions yield radiation directivities that peak in the upstream direction, but also exhibit substantial levels in directions normal to the wall, consistent with the presence of a cavity monopole field. Although various details of the approach in [19,20] have been criticized and subjected to modification, for example by Ekaterinaris [21] and by Shen and Sorensen [22], the general characteristics of the predicted radiation are probably correct in an overall sense, if not in detail. Indeed, they accord with later numerical studies (also based on an initial determination of an incompressible approximation of the cavity flow) by Grace et al. [23] and by Curtis Granda [24], that similarly predict large amplitude radiation normal to the wall.

The purpose of the present paper is to resolve these apparent inconsistencies between numerical and analytical predictions at low Mach numbers. It will be shown that the low Mach number dipole radiation, peaking in directions upstream and downstream of the cavity, is indeed the dominant source at very low Mach numbers, typically much smaller than $M=0.1$, however. Thus, it is this source that determines cavity radiation in underwater applications (where $M\sim0.01$) provided, of course, that the cavity walls are sufficiently 'rigid' to preclude monopole sources produced by pulsations in the cavity volume. But, when $M\sim0.1$ we shall show that the cavity 'Helmholtz' mode, although very weak and formally vanishingly small as $fL/U\to0$,

supplies an additional, omni-directional contribution that can exceed the drag dipole radiation over a range of frequencies. Furthermore, it will be shown that the monopole and dipole source strengths are *both* determined at low Mach numbers by the cavity drag fluctuations.

The low Mach number analysis will be framed, in terms of the theory of vortex sound [3], and the relevant equations are recalled in Section 2. The possible source types are identified by introducing an acoustic Green's function that is valid in the presence of low Mach number mean stream flow past the cavity (Section 3). At very low Mach numbers the acoustic amplitudes are always small enough for incompressible flow to be regarded as an excellent first approximation to the motion in the cavity. This flow determines the effective vortex sound source strengths, irrespective of whether the flow is characterized as 'shear layer' or 'wake' mode. Predictions of the theory are therefore illustrated in Section 4 for the simpler case of shear mode flow by means of an idealized model of shear layer excitation.

2. Formulation

Consider nominally steady, low Mach number, high Reynolds number mean flow in the positive x_1 direction of the rectangular coordinates (x_1, x_2, x_3) over the rectangular wall cavity of Fig. 1. The wall and the interior surfaces of the cavity are assumed to be rigid. The fluid has mean density and sound speed, respectively, equal to ρ_0, c_0, and the velocity in the main stream is U. The cavity has depth d and breadth b, and is aligned with its remaining side of length L parallel to the mean flow. The co-ordinate origin is taken at O in the plane of the wall at the center of the cavity mouth, with the x_2-axis normal to the wall and directed into the main stream.

Sound is produced by flow instability in the neighborhood of the cavity. According to Lighthill's acoustic analogy [3], when the total enthalpy B, say, is taken as the acoustic variable, the radiation can be expressed in terms of sources that represent excitation by vorticity and entropy fluctuations. For a nominally homogeneous flow at low Mach numbers the motion may be regarded as homentropic to a good approximation [25]. In that case the total enthalpy becomes

$$B = \int \frac{\mathrm{d}p}{\rho} + \tfrac{1}{2}v^2, \tag{3}$$

where ρ is fluid density, $p \equiv p(\rho)$ the pressure, and $\mathbf{v}$ denotes velocity, and Lighthill's acoustic analogy equation becomes

$$\left(\frac{D}{Dt}\left(\frac{1}{c^2}\frac{D}{Dt}\right) - \frac{1}{\rho}\nabla\cdot(\rho\nabla)\right)B = \frac{1}{\rho}\,\mathrm{div}(\rho\boldsymbol{\omega}\wedge\mathbf{v}), \tag{4}$$

where c is the local speed of sound. In the irrotational acoustic far field, Crocco's form of the momentum equation $\partial\mathbf{v}/\partial t = -\nabla B$ implies that $B = -\partial\varphi/\partial t$, where $\varphi(\mathbf{x}, t)$ is the velocity potential that determines the whole motion in the irrotational regions of the fluid. B is therefore equal to a *constant* in a steady mean flow, and at large distances from the sources perturbations in B represent outgoing sound waves.

In the particular case of low Mach number flow, when $M = U/c_0$ is smaller than about 0.2, say, so that $M^2 \ll 1$, the characteristics of the motion within and close to the cavity will be essentially the same as if the fluid is incompressible, the acoustic component constituting a very small

perturbation about this motion. We can then replace ρ and c where they occur explicitly in Eq. (4) by their respective mean values ρ_0 and c_0. On the left hand side we can also introduce the approximation (valid to first order in M)

$$\frac{1}{c_0^2}\frac{D^2}{Dt^2}\approx\frac{1}{c_0^2}\frac{\partial^2}{\partial t^2}+\frac{2}{c_0^2}\mathbf{U}_0\cdot\nabla\frac{\partial}{\partial t},$$

where $\mathbf{U}_0\equiv\mathbf{U}_0(\mathbf{x})$ is the undisturbed local mean velocity, which satisfies $\mathbf{U}_0\to(U,0,0)$ as $|\mathbf{x}|\to\infty$.

Eq. (4) accordingly reduces to

$$\left\{\frac{1}{c_0^2}\left(\frac{\partial^2}{\partial t^2}+2\mathbf{U}_0\cdot\nabla\frac{\partial}{\partial t}\right)-\nabla^2\right\}B=\mathrm{div}(\boldsymbol{\omega}\wedge\mathbf{v}). \tag{5}$$

At large distances from the cavity fluctuations in $B\equiv B(\mathbf{x},t)$ represent outgoing sound waves generated by the vortex source on the right of Eq. (5) and by its interactions with the cavity. B may therefore be assumed to vanish in the absence of radiation from the cavity, in which case if $p(\mathbf{x},t)$ now represents the perturbation pressure, it is readily deduced from Eq. (3) that in the acoustic far field (Ref. [3, p. 161]),

$$p=\frac{\rho_0 B}{(1+M\cos\theta)},\quad |\mathbf{x}|\to\infty\quad\text{where }\cos\theta=\frac{x_1}{|\mathbf{x}|}. \tag{6}$$

3. Solution of the aerodynamic sound equation

3.1. Green's function

The steady mean velocity $\mathbf{U}_0(\mathbf{x})$ must be irrotational in the absence of sound production at the cavity. When $M^2\ll 1$, it may be assumed to represent an incompressible flow whose details near the cavity depend on cavity geometry. To define this flow we introduce the Kirchhoff vector $\mathbf{X}(\mathbf{x})=(X_1(\mathbf{x}),0,X_3(\mathbf{x}))$ for the cavity, where X_j $(j=1,3)$ is the solution of following potential flow problem:

$$\nabla^2 X_j=0,\quad X_j\to x_j\quad\text{as }|\mathbf{x}|\to\infty,\quad \frac{\partial X_j}{\partial x_n}=0\quad\text{on } S, \tag{7}$$

where S is the rigid boundary consisting of the wall and cavity surfaces, and x_n is distance measured in the normal direction from S. X_j $(\mathbf{x})$ $(j=1,3)$ is just the velocity potential of flow over the cavity in the j direction that has unit speed in the j direction at large distances from the cavity.

Then the mean flow velocity $\mathbf{U}_0=U\nabla X_1(\mathbf{x})$, which can also be written as

$$\mathbf{U}_0=\nabla\{\mathbf{U}\cdot\mathbf{X}(\mathbf{x})\}\quad\text{where }\mathbf{U}=(U,0,0). \tag{8}$$

To determine the solution of the aerodynamic sound equation (5) when $\mathbf{U}_0$ is defined in this way we consider first the Green's function $G(\mathbf{x},\mathbf{y},t-\tau)$, which is the solution with outgoing wave behavior when the right hand side of Eq. (5) is replaced by the point source $\delta(\mathbf{x}-\mathbf{y})\delta(t-\tau)$. Because $B=-\partial\varphi/\partial t$ for irrotational motions, Green's function G is required to have vanishing

normal derivative on S. Introduce the transformation [3,26]

$$G(\mathbf{x},\mathbf{y},t-\tau) = -\frac{1}{2\pi}\int_{-\infty}^{\infty} \hat{G}(\mathbf{x},\mathbf{y},\omega)\mathrm{e}^{-\mathrm{i}\omega(t-\tau+\mathbf{M}\cdot(\mathbf{X}-\mathbf{Y})/c_0)}\,\mathrm{d}\omega, \tag{9}$$

where $\mathbf{M} = \mathbf{U}/c_0$, and $\mathbf{Y} = (Y_1, 0, Y_3)$ is the Kirchhoff vector expressed in terms of $\mathbf{y}$, then when $M^2 \ll 1$, $\hat{G}$ satisfies

$$(\nabla^2 + \kappa_0^2)\hat{G} = \delta(\mathbf{x}-\mathbf{y}), \quad \frac{\partial \hat{G}}{\partial x_n} = 0 \text{ on } S, \tag{10}$$

where $\kappa_0 = \omega/c_0$ is the acoustic wave number.

In the cavity radiation problem the source point $\mathbf{y}$ is within or near the cavity, and the observation point $\mathbf{x}$ is in the main stream, at large distances from the cavity. In these circumstances an analytical approximation to the solution of Eq. (10) can be derived by a familiar procedure [3] that involves a straightforward application of the reciprocal theorem $\hat{G}(\mathbf{x},\mathbf{y},\omega) = \hat{G}(\mathbf{y},\mathbf{x},\omega)$ [27]: the roles of $\mathbf{x}$ and $\mathbf{y}$ are interchanged in Eq. (10), which is now to be solved *as a function of* $\mathbf{y}$ for the reciprocal configuration in which the source is placed at the far field point $\mathbf{x}$. The distant source generates a spherical wave that may be regarded as locally plane when it arrives at the wall cavity. This greatly simplifies the problem when the characteristic wavelength $\sim 2\pi/\kappa_0$ of the sound is large compared to the typical cavity dimension, which is the case at sufficiently small Mach numbers. We can then anticipate that there are two principal contributions to the cavity response to the impinging wave: a monopole component produced by a periodic volume flux across the plane of the cavity mouth, corresponding to 'breathing' oscillations in the manner of a Helmholtz resonator [27], and a dipole field, with dipole axis parallel to the plane of the wall, representing an unsteady drag force on the cavity.

Therefore, in the usual way [3] for $\mathbf{y}$ within and near the cavity and $|\mathbf{x}| \to \infty$, we put

$$\hat{G} \approx \hat{G}_0 + \hat{G}_M + \hat{G}_D, \tag{11}$$

where $\hat{G}_0$ represents the uniform pressure produced by the incident wave in the neighborhood of the cavity, and $\hat{G}_M$ and $\hat{G}_D$, respectively, represent the monopole and dipole fields near the cavity.

In the absence of the cavity the exact Green's function is

$$\hat{G} = -\frac{\mathrm{e}^{\mathrm{i}\kappa_0|\mathbf{x}-\mathbf{y}|}}{4\pi|\mathbf{x}-\mathbf{y}|} - \frac{\mathrm{e}^{\mathrm{i}\kappa_0|\bar{\mathbf{x}}-\mathbf{y}|}}{4\pi|\bar{\mathbf{x}}-\mathbf{y}|}, \quad \bar{\mathbf{x}} = (x_1, -x_2, x_3), \tag{12}$$

which satisfies $\partial\hat{G}/\partial y_2 = 0$ on the plane surface $y_2 = 0$ of the wall. When $\kappa_0|\mathbf{y}| \ll 1$ and $\kappa_0|\mathbf{x}| \gg 1$ this becomes

$$\hat{G} \approx -\frac{\mathrm{e}^{\mathrm{i}\kappa_0|\mathbf{x}|}}{2\pi|\mathbf{x}|} + \frac{\mathrm{i}\kappa_0(\mathbf{x}+\bar{\mathbf{x}})\cdot\mathbf{y}\ \mathrm{e}^{\mathrm{i}\kappa_0|\mathbf{x}|}}{4\pi|\mathbf{x}|^2} + \ldots, \tag{13}$$

where the terms omitted are of order $\sim(\kappa_0|\mathbf{y}|)^2$ and smaller. The first term on the right hand side represents (as a function of $\mathbf{y}$) a uniform pressure fluctuation over the mouth of the cavity and must therefore correspond to $\hat{G}_0$. The second term $\sim O(\kappa_0|\mathbf{y}|)$, and satisfies as a function of $\mathbf{y}$ Laplace's equation to this order. It is the velocity potential of a uniform, incompressible flow parallel to the wall (because $\mathbf{x}+\bar{\mathbf{x}} = 2(x_1, 0, x_3)$), and must be augmented by a suitable solution of Laplace's equation that accounts for the presence of the cavity (and in particular for the singular

behavior of $\hat{G}$ near the cavity edges) and describes the diversion of this flow into and out of the cavity mouth. Definition (7) of the Kirchhoff vector enables this to be accomplished simply by replacing $(\mathbf{x}+\bar{\mathbf{x}})\cdot\mathbf{y}$ by $(\mathbf{x}+\bar{\mathbf{x}})\cdot\mathbf{Y}\equiv 2\mathbf{x}\cdot\mathbf{Y}$.

Thus,

$$\hat{G}_0=-\frac{e^{ik_0|\mathbf{x}|}}{2\pi|\mathbf{x}|},\quad \hat{G}_D=\frac{ik_0\mathbf{x}\cdot\mathbf{Y}e^{ik_0|\mathbf{x}|}}{2\pi|\mathbf{x}|^2}, \tag{14}$$

and it remains to determine $\hat{G}_M$.

The uniform incident applied pressure distribution $\hat{G}_0$ over the mouth of a cavity of depth d produces vertically orientated compressional motions described by the following representations:

$$\hat{G}=\alpha\cos\{k_0(y_2+d)\}\quad \text{within the cavity in } -d<y_2<0, \tag{15}$$

$$\hat{G}_M=\begin{cases}\beta\varphi^*(\mathbf{y})+\gamma & \text{in the cavity mouth } y_2\sim 0,\\ -\dfrac{\delta\mathscr{A}}{2\pi|\mathbf{y}|}e^{ik_0|\mathbf{y}|} & \text{in free space above the cavity } y_2\gg L,\end{cases} \tag{16}$$

where $\alpha,\beta,\gamma,\delta$ are constant coefficients, $\mathscr{A}=bL$ is the area of the cavity mouth, and $\varphi^*(\mathbf{y})$ is the solution of Laplace's equation describing uniform flow from the mouth, normalized such that

$$\varphi^*(\mathbf{y})\sim-\frac{\mathscr{A}}{2\pi|\mathbf{y}|}\quad |\mathbf{y}|\gg d \quad \text{above the cavity,} \tag{17}$$

$$\sim y_2-\ell,\quad y_2\to -d \quad \text{within the cavity,} \tag{18}$$

where $\ell\sim\sqrt{\pi\mathscr{A}/4}$ is the 'end correction' of the mouth [3,27].

Equations determining the values of the coefficients $\alpha,\beta,\gamma,\delta$ are obtained by matching the various representations of $\hat{G}$ and $\hat{G}_M$. Thus, in the region $k_0|\mathbf{y}|\ll 1$ just above the cavity mouth, Eqs. (16) and (17) imply that

$$-\frac{\beta\mathscr{A}}{2\pi|\mathbf{y}|}+\gamma\equiv-\frac{\delta\mathscr{A}}{2\pi|\mathbf{y}|}-\frac{i\delta k_0\mathscr{A}}{2\pi}$$

from which it follows that $\delta=\beta$ and $\gamma=-i\beta k_0\mathscr{A}/2\pi$, and therefore that

$$\hat{G}_M=\beta\left(\varphi^*(\mathbf{y})-\frac{ik_0\mathscr{A}}{2\pi}\right)\quad \text{in the cavity mouth.} \tag{19}$$

Similarly within the cavity, representation (15) must match just below the cavity mouth with the continuation of $\hat{G}=\hat{G}_0+\hat{G}_M+\hat{G}_D$ given by Eqs. (14) and (19). Now $\mathbf{Y}$ must decrease exponentially fast with distance into the cavity [28, Section 66], and therefore (using Eqs. (15) and (18))

$$\alpha\cos(k_0d)-\alpha k_0y_2\sin(k_0d)\equiv\beta\left(y_2-\ell-\frac{ik_0\mathscr{A}}{2\pi}\right)+\hat{G}_0,$$

from which it follows, in particular, that

$$\hat{G}_M \approx \left(\varphi^*(\mathbf{y}) - \frac{\mathrm{i}\kappa_0\mathscr{A}}{2\pi}\right)\frac{\mathrm{e}^{\mathrm{i}\kappa_0|\mathbf{x}|}}{2\pi|\mathbf{x}|}\Big/\left(\frac{1}{\kappa_0\tan(\kappa_0 d)} - \ell - \frac{\mathrm{i}\kappa_0\mathscr{A}}{2\pi}\right)$$

$$\approx \left(\varphi^*(\mathbf{y}) - \frac{\mathrm{i}\kappa_0\mathscr{A}}{2\pi}\right)\frac{\kappa_0\sin(\kappa_0 d)}{\cos\{\kappa_0(d+\ell+\mathrm{i}\kappa_0\mathscr{A}/2\pi)\}}\frac{\mathrm{e}^{\mathrm{i}\kappa_0|\mathbf{x}|}}{2\pi|\mathbf{x}|}. \tag{20}$$

The steps in the derivation of this approximation for $\hat{G}_M$ are strictly valid only for a deep cavity (so that $\kappa_0\ell, \kappa_0^2\mathscr{A}/2\pi \ll 1$), but if necessary it may be assumed that the values of ℓ and $\mathscr{A}$ are suitably adjusted to ensure the validity of the second line of Eq. (20). The depth mode resonance frequencies are determined by the zeros of the cosine term in the denominator of the second line of Eq. (20). The lowest order mode occurs at the complex frequency satisfying

$$\kappa_0\left(d+\ell+\frac{\mathrm{i}\kappa_0\mathscr{A}}{2\pi}\right) = \frac{\pi}{2},$$

that is for

$$\kappa_0 d \sim \frac{\pi d}{2(d+\ell)} - \frac{\mathrm{i}\pi\mathscr{A}d}{8(d+\ell)^3}. \tag{21}$$

The real part is the usual expression for the lowest order depth mode for a cavity whose depth d is augmented by the end correction ℓ, which represents the effective length by which the cavity must be extended to account for the inertia of fluid above the mouth of the cavity also set into reciprocating motion by the cavity resonance; the imaginary part accounts for the damping of this mode by radiation into the fluid.

Tam [29] has shown for the case of *two-dimensional* rectangular cavities that the frequency of the lowest order mode is well represented by Eq. (21) even for d/L as small as 1, for a suitable choice of the value of ℓ. For deep cavities we can use Rayleigh's [27] approximation

$$\ell \sim \frac{\sqrt{\pi\mathscr{A}}}{4}. \tag{22}$$

For the purpose of the numerical illustrations given below for the moderately shallow case of $d/L = 0.5$ it will be sufficient to use Eq. (22)—in practice precise values of ℓ can always be derived from a numerical simulation of the acoustic mode.

The complex factor in the argument of the cosine term in Eq. (20) increases rapidly with κ_0, showing that higher order modes of the cavity are strongly damped by radiation losses. Thus, we can anticipate that only the lowest order 'Helmholtz resonator' mode (21) of the cavity will be of any importance in applications to cavity flow-noise, although this is not persued further here.

Hence, substituting Eqs. (14) and (20) in Eq. (11), and using the inversion formula (9), it follows that for $\mathbf{y}$ in the neighborhood of the cavity mouth and $\mathbf{x}$ in the acoustic far field,

$$G(\mathbf{x},\mathbf{y},t-\tau)\approx -\frac{1}{2\pi}\int_{-\infty}^{\infty}(\hat{G}_0+\hat{G}_M+\hat{G}_D)(\mathbf{x},\mathbf{y},\omega)\,\mathrm{e}^{-\mathrm{i}\omega(t-\tau+\mathbf{M}\cdot(\mathbf{X}-\mathbf{Y})/c_0)}\,\mathrm{d}\omega$$
$$=\frac{1}{(2\pi)^2|\mathbf{x}|}\int_{-\infty}^{\infty}\left\{1-\left(\varphi^*(\mathbf{y})-\frac{\mathrm{i}\kappa_0\mathscr{A}}{2\pi}\right)\frac{\kappa_0\sin(\kappa_0 d)}{\cos\{\kappa_0(d+\ell+\mathrm{i}\kappa_0\mathscr{A}/2\pi)\}}\right.$$
$$\left.-\frac{\mathrm{i}\kappa_0\mathbf{x}\cdot\mathbf{Y}}{|\mathbf{x}|}\right\}\mathrm{e}^{-\mathrm{i}\omega(t-\tau-|\mathbf{x}|/c_0+\mathbf{M}\cdot(\mathbf{X}-\mathbf{Y})/c_0)}\,\mathrm{d}\omega. \tag{23}$$

To interpret this result, observe first that cavity resonance corresponds to $\kappa_0 d\sim O(1)$. At such frequencies the second term in the brace brackets of the integrand, involving $\mathbf{Y}$, is not important. The latter becomes significant away from resonances, and then only when the source point $\mathbf{y}$ is close to a cavity edge. The basic assumption is that very high frequencies (in excess of the first cavity resonance) are irrelevant, and this will be the case when excitation occurs at low Mach numbers.

3.2. The radiated sound

Green's function (23) now permits the solution of the aerodynamic sound equation (5) , where B is given by Eq. (6) in the far field, to be expressed in the form [3]

$$p\approx\frac{-\rho_0}{(1+M\cos\theta)}\int(\boldsymbol{\omega}\wedge\mathbf{v})(\mathbf{y},\tau)\cdot\frac{\partial G}{\partial\mathbf{y}}(\mathbf{x},\mathbf{y},t-\tau)\,\mathrm{d}^3\mathbf{y}\,\mathrm{d}\tau,\quad |\mathbf{x}|\to\infty, \tag{24}$$

where the integration is over all values of the retarded time τ and the fluid region where the vorticity $\boldsymbol{\omega}\neq\mathbf{0}$. There are no contributions from surface integrals over the wall and cavity, on which the fluid normal component of velocity and the normal derivative of G both vanish.

It follows from this result that only the $\mathbf{y}$-dependent part of the Green's function (23) need be used in Eq. (24). Therefore, for small Mach numbers and an acoustically compact source flow, the acoustic pressure given by Eq. (24) can be reduced to the form

$$p\approx\frac{\rho_0}{(2\pi)^2(1+M\cos\theta)|\mathbf{x}|}\int(\boldsymbol{\omega}\wedge\mathbf{v})(\mathbf{y},\tau)\cdot\frac{\partial}{\partial\mathbf{y}}\int_{-\infty}^{\infty}\left\{\frac{\varphi^*(\mathbf{y})\,\kappa_0\sin(\kappa_0 d)}{\cos\{\kappa_0(d+\ell+\mathrm{i}\kappa_0\mathscr{A}/2\pi)\}}\right.$$
$$\left.+\mathrm{i}\kappa_0\left(\frac{\mathbf{x}}{|\mathbf{x}|}-\mathbf{M}\right)\cdot\mathbf{Y}\right\}\mathrm{e}^{-\mathrm{i}\omega\{t-\tau-(|\mathbf{x}|-\mathbf{M}\cdot\mathbf{x})/c_0\}}\,\mathrm{d}\omega\,\mathrm{d}^3\mathbf{y}\,\mathrm{d}\tau,\quad |\mathbf{x}|\to\infty. \tag{25}$$

3.3. Leading edge Kutta condition

In a typical oscillatory cavity flow the region within, above and downstream of the cavity is filled with vorticity generated by shedding, principally from the leading edge region of the cavity. The length scales of the unsteady hydrodynamic motions induced by this vorticity are comparable to the cavity length L, but the characteristic extent of a coherent region of vorticity is usually very much smaller. This means that the main contributions to the volume integral in Eq. (25) are from those regions where $\nabla\varphi^*$ and ∇Y_j $(j=1,3)$ vary rapidly, since $\int(\boldsymbol{\omega}\wedge\mathbf{v})(\mathbf{y},\tau)\,\mathrm{d}^3\mathbf{y}\sim\mathbf{0}$ in regions

where $\nabla\varphi^*$ and ∇Y_j can be regarded as constant or as varying very slowly relative to the length scale of the vorticity.

It follows that the cavity *edges* at which $\nabla\varphi^*$ and ∇Y_j become infinite are the main sources of the cavity radiation, and a good estimate of the value of the integral can therefore be obtained by expanding these derivatives about these edges. In doing this we can explicitly discard any contributions from the *leading edge* of the cavity, because the Kutta condition ensures that acoustic excitation by cavity vorticity interacting with this edge is inhibited by the shedding of fresh vorticity [2,3,30–32]. Similarly, the contributions from the side edges of the cavity (parallel to the mean flow direction) are small, because the vortex source $\boldsymbol{\omega}\wedge\mathbf{v}$ convects predominantly in the mean flow direction so that its interaction with the edge is effectively invariant with time (i.e. it is 'silent'). We therefore conclude, in accordance with all previous observations, that it is primarily the trailing edge of the cavity that is responsible for the radiated sound.

Recall that Y_j $(j=1,3)$ may be interpreted as the velocity potential of a uniform flow over the cavity in the j-direction. This means that $|\nabla Y_3|\ll|\nabla Y_1|$ at the cavity trailing edge, and therefore that the contribution from Y_3 in Eq. (25) can be discarded. If we now introduce a 'strip theory' approximation for Y_1 in the immediate vicinity of the edge, by equating it to the corresponding velocity potential for flow over a two-dimensional cavity, which is readily found by conformal mapping, we find (for details see Ref. [3])

$$Y_1(\mathbf{y})\sim C_1L^{1/3}\mathrm{Re}(z^{2/3})\quad\text{where } z=y_1-\frac{L}{2}+\mathrm{i}y_2 \text{ and } C_1=\frac{3}{2}\left[\frac{(1-\mu)}{6E(\mu)}\right]^{1/3}, \tag{26}$$

where μ is the solution of the equation

$$\frac{K(1-\mu)-E(1-\mu)}{E(\mu)}=\frac{d}{L} \tag{27}$$

and $K(\xi)=\int_0^{\pi/2}\mathrm{d}\lambda/\sqrt{1-\xi\sin^2\lambda}$, $E(\xi)=\int_0^{\pi/2}\sqrt{1-\xi\sin^2\lambda}\,\mathrm{d}\lambda$ $(0<\xi<1)$ are complete elliptic integrals [33].

A similar strip-theory calculation reveals that near the trailing edge

$$\varphi^*(\mathbf{y})\sim C_2\,Y_1(\mathbf{y}),\quad C_2=2\left[\frac{E(\mu)}{4\pi(1-\mu)}\right]^{1/3}. \tag{28}$$

Hence, Eq. (25) becomes

$$\begin{aligned}p\approx{}&\frac{\rho_0}{(2\pi)^2(1+M\cos\theta)|\mathbf{x}|}\int(\boldsymbol{\omega}\wedge\mathbf{v})(\mathbf{y},\tau)\cdot\frac{\partial Y_1}{\partial\mathbf{y}}(\mathbf{y})\,\mathrm{d}^3\mathbf{y}\\&\times\int_{-\infty}^{\infty}\kappa_0\left(\frac{C_2\sin(\kappa_0 d)}{\cos\{\kappa_0(d+\ell+\mathrm{i}\kappa_0\mathscr{A}/2\pi)\}}\right.\\&\left.+\mathrm{i}(\cos\theta-M)\right)\mathrm{e}^{-\mathrm{i}\omega\{t-\tau-(|\mathbf{x}|-\mathbf{M}\cdot\mathbf{x})/c_0\}}\,\mathrm{d}\omega\,\mathrm{d}\tau,\quad|\mathbf{x}|\to\infty,\end{aligned} \tag{29}$$

where Y_1 is given by Eq. (26).

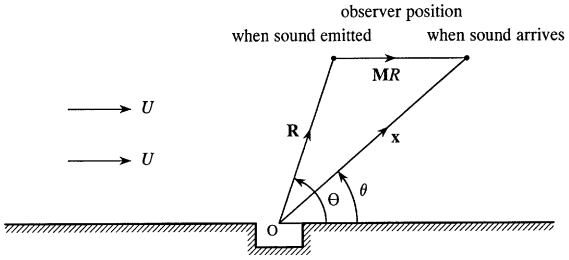

Fig. 2. Illustrating the relation between the co-ordinate systems **x** and **R**.

3.4. Physical interpretation

The first and second terms in the large brackets of Eq. (29) correspond respectively to monopole and dipole radiation from the cavity. The monopole character of the first term should be obvious from the discussion in Section 3.1. To understand the dipole nature of the second term note first that Eq. (29) is the acoustic pressure as measured by an observer *fixed relative to the cavity*, and therefore moving at speed U in the negative x_1 direction relative to the mean stream. Let **R** be the vector position relative to the cavity of an observer in a reference frame moving with the fluid *at the time of emission* of the arriving sound. For such an observer the cavity appears to translate at speed U in the negative x_1 direction. The co-ordinate systems **x** and **R** are related by (see Fig. 2) $\mathbf{x} = \mathbf{R} + \mathbf{M}R$, since an observer fixed relative to the fluid moves a distance $U \times (R/c_0)$ in the x_1 direction relative to the cavity during the time of travel R/c_0 of the sound from the cavity to the observer. The following relations are now easily derived for small M:

$$|\mathbf{x}| - \mathbf{M}\cdot\mathbf{x} = |\mathbf{R}|, \quad |\mathbf{x}| = |\mathbf{R}|(1 + M\cos\Theta), \quad \cos\theta - M = \frac{\cos\Theta}{(1 + M\cos\Theta)}, \tag{30}$$

where Θ is the angle between the observer direction and the mean flow direction at the time of emission of the sound.

Making these substitutions in Eq. (29) we find, for small M,

$$\begin{aligned} p \approx{}& \frac{\rho_0}{(2\pi)^2(1 + M\cos\Theta)^2|\mathbf{R}|}\int(\boldsymbol{\omega}\wedge\mathbf{v})(\mathbf{y},\tau)\cdot\frac{\partial Y_1}{\partial\mathbf{y}}(\mathbf{y})\,\mathrm{d}^3\mathbf{y} \\ &\times\int_{-\infty}^{\infty}\kappa_0\left(\frac{C_2\sin(\kappa_0 d)}{\cos\{\kappa_0(d + \ell + \mathrm{i}\kappa_0\mathscr{A}/2\pi)\}} + \frac{\mathrm{i}\cos\Theta}{(1 + M\cos\Theta)}\right) \\ &\times \mathrm{e}^{-\mathrm{i}\omega\{t-\tau-|\mathbf{R}|/c_0\}}\,\mathrm{d}\omega\,\mathrm{d}\tau, \quad |\mathbf{R}|\to\infty, \end{aligned} \tag{31}$$

where Y_1 is given by Eq. (26). This formula represents the radiation measured by a fixed observer from a uniformly translating cavity as being equal to the sum of a monopole amplified by the familiar two powers of the Doppler factor $1/(1 + M\cos\Theta)$ together with a surface interaction dipole magnified by three Doppler factors (cf. [34]).

The strengths of the monopole and dipole sources are both determined by the value of the integral

$$F(\tau) = \rho_0\int(\boldsymbol{\omega}\wedge\mathbf{v})(\mathbf{y},\tau)\cdot\frac{\partial Y_1}{\partial\mathbf{y}}(\mathbf{y})\,\mathrm{d}^3\mathbf{y}, \tag{32}$$

which is just the force exerted on the cavity in the x_1 direction (i.e. the cavity *drag*) when the unsteady flow in the vicinity of the cavity is regarded as incompressible [3]. Only the *unsteady* component of the drag actually contributes to the radiation, and it may therefore be assumed that the mean component of the drag has been excluded, and that henceforth $F(t)$ refers only to the fluctuating part, having zero mean value. Then, for example, Eq. (29) becomes

$$p \approx \frac{1}{2\pi(1+M\cos\theta)|\mathbf{x}|}\int_{-\infty}^{\infty}\hat{F}(\omega)\kappa_0\left(\frac{C_2\sin(\kappa_0 d)}{\cos\{\kappa_0(d+\ell+\mathrm{i}\kappa_0\mathscr{A}/2\pi)\}}+\mathrm{i}(\cos\theta-M)\right)$$
$$\times\, \mathrm{e}^{-\mathrm{i}\omega\{t-(|\mathbf{x}|-\mathbf{M}\cdot\mathbf{x})/c_0\}}\,\mathrm{d}\omega, \quad |\mathbf{x}|\to\infty, \tag{33}$$

where

$$\hat{F}(\omega)=\frac{1}{2\pi}\int_{-\infty}^{\infty}F(t)\mathrm{e}^{\mathrm{i}\omega t}\,\mathrm{d}t \tag{34}$$

is the Fourier transform of the fluctuating drag.

4. Numerical illustration

4.1. Acoustic pressure frequency spectrum

The unsteady drag $F(t)$ may be assumed to be a stationary random function of the time, whose ('two-sided') spectrum $\Psi(\omega)$, say, satisfies

$$\langle F(\omega)F^*(\omega')\rangle = \Psi(\omega)\delta(\omega-\omega'), \tag{35}$$

where the angle brackets $\langle\ \rangle$ represent a time or ensemble average, and the asterisk denotes complex conjugate. For the low Mach number flows encompassed by the present theory $\Psi(\omega)$ can be found from measurement or by numerical simulation of the essentially incompressible cavity flow. When known it can be used in conjunction with Eq. (33) to calculate the farfield acoustic pressure frequency spectrum, which will be denoted by $\Phi(\omega,\mathbf{x})$, and defined such that

$$\langle p^2(\mathbf{x},t)\rangle = \int_0^{\infty}\Phi(\omega,\mathbf{x})\,\mathrm{d}\omega. \tag{36}$$

Thus, using Eq. (33) and definition (35), we find

$$\Phi(\omega,\mathbf{x})\approx\frac{\Psi(\omega)\kappa_0^2}{2\pi^2(1+M\cos\theta)^2|\mathbf{x}|^2}\left|\frac{C_2\sin(\kappa_0 d)}{\cos\{\kappa_0(d+\ell+i\kappa_0\mathscr{A}/2\pi)\}}+\mathrm{i}(\cos\theta-M)\right|^2, \quad |\mathbf{x}|\to\infty. \tag{37}$$

This formula gives the frequency dependence with respect to an observer fixed relative to the cavity. If the cavity is attached to a moving body, and the observer is at rest relative to the fluid, the observed frequency Ω will have the Doppler shifted value

$$\Omega=\frac{\omega}{1+M\cos\Theta}, \tag{38}$$

so that if $\langle p^2(\mathbf{R},t)\rangle = \int_0^\infty \Phi(\Omega,\mathbf{R})\,\mathrm{d}\Omega$, then

$$\Phi(\Omega,\mathbf{R}) \approx \frac{\Psi(\omega)\kappa_0^2}{2\pi^2(1+M\cos\Theta)^3|\mathbf{R}|^2}\left|\frac{C_2\sin(\kappa_0 d)}{\cos\{\kappa_0(d+\ell+\mathrm{i}\kappa_0\mathscr{A}/2\pi)\}}+\frac{\mathrm{i}\cos\Theta}{(1+M\cos\Theta)}\right|^2, \quad |\mathbf{R}|\to\infty, \quad (39)$$

in which ω and $\kappa_0=\omega/c_0$ are defined in terms of Ω as in Eq. (38).

4.2. Analytical model for shear layer mode radiation

To illustrate predictions of Eq. (37) a simple yet mathematically tractable model will now be considered for a shallow cavity subject to shear layer mode excitation. The principal aerodynamic sources $\mathrm{div}(\boldsymbol{\omega}\wedge\mathbf{v})$ on the right of Eq. (5) are then confined to the region above the cavity mouth. In a first approximation the flow is parallel to the x_1 direction, so that the main contribution to the drag integral (32) (wherein Y_1 is given approximately by Eq. (26)) is determined by the *spanwise* component ω_3 of the vorticity.

We therefore write

$$(\boldsymbol{\omega}\wedge\mathbf{v})(\mathbf{y},\tau)\approx\mathbf{j}\int_{-\infty}^{\infty}\mathscr{F}(k,k_\perp,\omega,y_2)\mathrm{e}^{\mathrm{i}(ky_1+k_\perp y_3-\omega\tau)}\,\mathrm{d}k\,\mathrm{d}k_\perp\,\mathrm{d}\omega, \quad y_2>0, \quad |y_3|<\frac{b}{2}, \quad (40)$$

where $\mathbf{j}$ is a unit vector in the x_2 direction, normal to the plane of the wall, and $\mathscr{F}(k,k_\perp,\omega,y_2)$ determines the distribution across the shear layer of harmonic constituents of the unsteady shear flow of frequency ω and with streamwise and spanwise wavelengths, respectively, equal to $2\pi/k$ and $2\pi/k_\perp$. Inserting this formula into the integral of Eq. (32), and using the local approximation (26) for Y_1, the y_1-integral is readily evaluated to yield the Fourier transform $\hat{F}(\omega)$ of the unsteady drag in the form

$$\hat{F}(\omega)=\frac{C_1\Gamma(\frac{2}{3})L^{1/3}}{\sqrt{3}}\rho_0\int\frac{\mathscr{F}(k,k_\perp,\omega,y_2)}{(k-i0)^{2/3}}\mathrm{e}^{\mathrm{i}(k_\perp y_3-\pi/3)-|k|y_2}\,\mathrm{d}k\,\mathrm{d}k_\perp\,\mathrm{d}y_2\,\mathrm{d}y_3, \quad (41)$$

where the notation '$-\mathrm{i}0$' implies that the branch cut for $(k-\mathrm{i}0)^{2/3}$ is to be taken from $k=0$ to $+\mathrm{i}\infty$ in the upper half-plane.

This result can be cast in a more useful form in terms of the hydrodynamic pressure fluctuations p_s, say, that the same flow would exert on the rigid wall *in the absence of the cavity*. This is usually called the 'blocked surface pressure', and in a first approximation may be identified with the (measurable) wall surface pressure fluctuations just downstream of the cavity. At low Mach numbers we can regard this pressure as that generated by the shear layer vorticity when the flow is incompressible, and it is therefore determined by the incompressible form of Eq. (4),

$$\nabla^2 B=-\mathrm{div}(\boldsymbol{\omega}\wedge\mathbf{v}), \quad x_2>0 \quad \text{where } p_s=\rho_0 B \text{ on } x_2=0. \quad (42)$$

When $\boldsymbol{\omega}\wedge\mathbf{v}$ is given by Eq. (40) a routine calculation [3] yields

$$p_s=\int_{-\infty}^{\infty}\hat{p}_s(k,k_\perp,\omega)\mathrm{e}^{\mathrm{i}(ky_1+k_\perp y_3-\omega t)}\,\mathrm{d}k\,\mathrm{d}k_\perp\,\mathrm{d}\omega, \quad (43)$$

where

$$\hat{p}_s(k,k_\perp,\omega)=\frac{\rho_0}{2}\int_0^\infty\mathscr{F}(k,k_\perp,\omega,y_2)\mathrm{e}^{-\{k^2+k_\perp^2\}^{1/2}y_2}\,\mathrm{d}y_2. \quad (44)$$

Now $k \sim \omega/U_c$ at those values of the wave number k where the blocked pressure Fourier amplitude $\hat{p}_s(k, k_\perp, \omega)$ is significant. Because the motion over the cavity can be regarded as locally two-dimensional, the corresponding typical values of the spanwise wave number $k_\perp \ll k$. Thus, $\{k^2 + k_\perp^2\}^{1/2}$ can be replaced by $|k|$ in the exponential of Eq. (44), and it is then deduced from Eq. (41) that

$$\hat{F}(\omega) \approx \frac{2C_1\Gamma(\frac{2}{3})L^{1/3}}{\sqrt{3}} \int \frac{\hat{p}_s(k, k_\perp, \omega)}{(k - \mathrm{i}0)^{2/3}} \mathrm{e}^{\mathrm{i}(k_\perp y_3 - \pi/3)}\, \mathrm{d}k\, \mathrm{d}k_\perp\, \mathrm{d}y_3. \tag{45}$$

For stationary random flow we also have [3]

$$\langle \hat{p}_s(k, k_\perp, \omega)\hat{p}_s^*(k', k'_\perp, \omega') \rangle = P(k, k_\perp, \omega)\delta(k - k')\delta(k_\perp - k'_\perp)\delta(\omega - \omega'), \tag{46}$$

where $P(k, k_\perp, \omega)$ is the blocked pressure wave number frequency spectrum. Hence, by forming the product $\langle \hat{F}(\omega)\hat{F}^*(\omega') \rangle$ from Eq. (45), using Eq. (46), and making the further assumption that the spanwise correlation length of the unsteady motions is small compared to the cavity width b, we deduce from definition (35), that

$$\Psi(\omega) \approx \frac{8\pi C_1^2\Gamma^2(\frac{2}{3})bL^{2/3}}{3} \int_{-\infty}^{\infty} \frac{P(k, 0, \omega)\, \mathrm{d}k}{|k|^{4/3}}, \tag{47}$$

and therefore that the far field acoustic pressure spectrum (37) can be written as

$$\Phi(\omega, \mathbf{x}) \approx \frac{4C_1^2\Gamma^2(\frac{2}{3})bL^{2/3}\kappa_0^2}{3\pi(1 + M\cos\theta)^2|\mathbf{x}|^2} \left| \frac{C_2 \sin(\kappa_0 d)}{\cos\{\kappa_0(d + \ell + \mathrm{i}\kappa_0\mathscr{A}/2\pi)\}} + \mathrm{i}(\cos\theta - M) \right|^2 \times \int_{-\infty}^{\infty} \frac{P(k, 0, \omega)\, \mathrm{d}k}{|k|^{4/3}}, \quad |\mathbf{x}| \to \infty. \tag{48}$$

The functional form of $P(k, 0, \omega)$ can, in principle, be estimated from measurements of the wall pressure fluctuations just downstream of the trailing edge of the cavity, provided it is permissible to assume that the statistical properties of the shear layer motions near the trailing edge of the cavity are well approximated by those immediately downstream of the cavity.

As an alternative approximate procedure, however, it will be assumed that $P(k, 0, \omega)$ is sharply peaked at $k = \omega/U_c$, which is the expected behavior when the dominant vortical disturbances convect at speed U_c. The integral in Eq. (48) may then be evaluated by replacing $|k|$ by ω/U_c in the denominator, and setting $\ell_3\Phi_{pp}(\omega)/\pi = \int_{-\infty}^{\infty} P(k, 0, \omega)\, \mathrm{d}k$, where $\Phi_{pp}(\omega)$ is the frequency spectrum of the wall blocked pressure fluctuations, and $\ell_3 \ll b$ is the spanwise correlation length. Therefore,

$$\Phi(\omega, \mathbf{x}) \approx \frac{4C_1^2\Gamma^2(\frac{2}{3})bL^{2/3}}{3\pi^2(1 + M\cos\theta)^2|\mathbf{x}|^2} \frac{\ell_3\kappa_0^2\Phi_{pp}(\omega)}{(\omega/U_c)^{4/3}} \left| \frac{C_2 \sin(\kappa_0 d)}{\cos\{\kappa_0(d + \ell + \mathrm{i}\kappa_0\mathscr{A}/2\pi)\}} + \mathrm{i}(\cos\theta - M) \right|^2, \quad |\mathbf{x}| \to \infty. \tag{49}$$

Consider a case (typical of low Mach number flow over a shallow cavity) where the pressure fluctuations near the cavity peak at the frequency of the second Rossiter mode, near $fL/U = 1$. Let the functional form of $\Phi_{pp}(\omega)$ be approximated by the following empirical formula [3] for

turbulent boundary layer flow:

$$\frac{\Phi_{pp}(\omega)(U/\delta_*)}{(\rho_0 v_*^2)^2} \approx \frac{(\omega\delta_*/U)^2}{\{(\omega\delta_*/U)^2+\alpha_p^2\}^{3/2}}, \quad \alpha_p = 0.12, \quad \ell_3 \approx \frac{1.4U_c}{\omega}. \tag{50}$$

In this formula δ_* is the effective displacement thickness of the boundary layer flow, but will be assigned the value

$$\delta_* = \frac{L\alpha_p}{\pi\sqrt{2}}, \tag{51}$$

to ensure that the spectral peak occurs at $f\,L/U = 1$. The velocity v_* is the nominal friction velocity of the wall flow, but its precise value is not required for the present illustrations.

In non-dimensional form we may now write

$$\frac{\Phi(\omega,\mathbf{x})(U/\delta_*)}{(\rho_0 v_*^2)^2(L/|\mathbf{x}|)^2}\Bigg/\frac{5.6C_1^2\Gamma^2(\frac{2}{3})}{3\pi^2}\left(\frac{\delta_*}{L}\right)^{1/3}\left(\frac{b}{L}\right)\left(\frac{U_c}{U}\right)^{7/3}$$
$$\approx \frac{M^2(\omega\delta_*/U)^{5/3}}{(1+M\cos\theta)^2\{(\omega\delta_*/U)^2+\alpha_p^2\}^{3/2}}\left|\frac{C_2\sin(\kappa_0 d)}{\cos\{\kappa_0(d+\ell+\mathrm{i}\kappa_0\mathscr{A}/2\pi)\}}+\mathrm{i}(\cos\theta-M)\right|^2. \tag{52}$$

Thus, the mean square acoustic pressure scales as $(\rho_0 U^2)^2 M^2$, and the overall acoustic intensity varies as $\rho_0 U^3 M^3$. This is the expected behavior for an aeroacoustic dipole source; in our case the source is modified by the cavity monopole, but we shall see below that the maximal strength of the monopole is of the same dipole order.

Typical plots of the far field acoustic spectrum

$$10\times\log_{10}\left\{\frac{\Phi(\omega,\mathbf{x})(U/\delta_*)}{(\rho_0 v_*^2)^2(L/|\mathbf{x}|)^2}\Bigg/\frac{5.6C_1^2\Gamma^2(\frac{2}{3})}{3\pi^2}\left(\frac{\delta_*}{L}\right)^{1/3}\left(\frac{b}{L}\right)\left(\frac{U_c}{U}\right)^{7/3}\right\}$$

are illustrated in Figs. 3 and 4, respectively, for $M = 0.01, 0.1$ in the radiation direction $\theta = 30^\circ$. It is assumed that

$$\frac{U_c}{U} = 0.5, \quad \frac{b}{L} = 1, \quad \frac{d}{L} = 0.5 \quad \text{for which } C_1 = 0.69,\ C_2 = 1.02. \tag{53}$$

Also shown for comparison is the model shear layer mode blocked pressure spectrum Φ_{pp} normalized as in Eq. (50), with a broad peak at the second Rossiter frequency ($f\,L/U \approx 1$).

The very low Mach number case $M = 0.01$ is characteristic of underwater applications, provided the cavity walls are sufficiently rigid that structurally driven cavity modes are not important. The monopole peak occurs at the relatively high Strouhal number $f\,L/U \sim 25$, and its contribution is smaller than that of the spectrum maximum near the Rossiter mode $f\,L/U = 1$. At Strouhal numbers less than 10, the radiation is dominated by the drag dipole source—Mach number ('Doppler') effects are unimportant when $M = 0.01$, and this implies that the radiation directivity has the usual dipole peaks in the upstream and downstream directions, and that there is a radiation null in the direction normal to the wall. In practice the source spectrum Φ_{pp} probably decays much faster than the boundary layer analog model (50) used in this calculation, and this would tend to suppress even further the higher frequency monopole radiation.

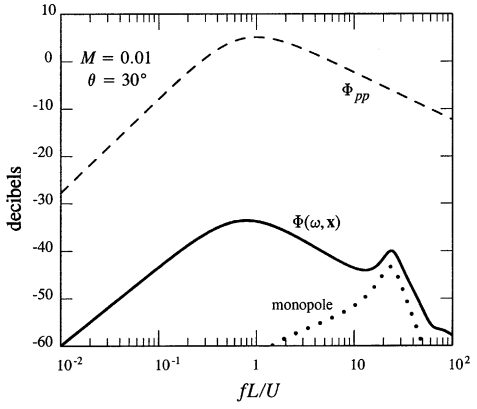

Fig. 3. Acoustic pressure spectrum $10\times\log_{10}\left\{\dfrac{\Phi(\omega,\mathbf{x})(U/\delta_*)}{(\rho_0 v_*^2)^2(L/|\mathbf{x}|)^2}\Big/\dfrac{5.6C_1^2\Gamma^2(\frac{2}{3})}{3\pi^2}\left(\dfrac{\delta_*}{L}\right)^{1/3}\left(\dfrac{U_c}{U}\right)^{7/3}\right\}$, (——) defined by Eq. (52) for conditions (53) when $M=0.01,\ \theta=30^\circ$. Also shown is the corresponding blocked pressure spectrum $10\times\log_{10}(\Phi_{pp}(U/\delta_*)/(\rho_0 v_*^2)^2)$ (- - - - , Eq. (50)) peaking at the second Rossiter mode $f\,L/U\sim 1$, and the cavity 'monopole' radiation (● ● ●).

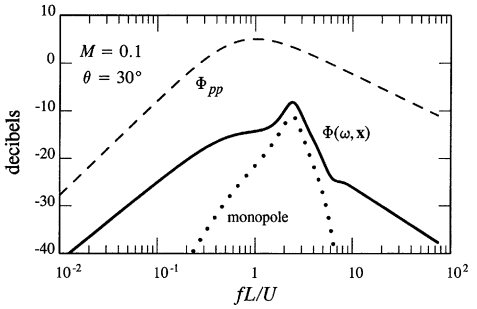

Fig. 4. Acoustic pressure spectrum $10\times\log_{10}\left\{\dfrac{\Phi(\omega,\mathbf{x})(U/\delta_*)}{(\rho_0 v_*^2)^2(L/|\mathbf{x}|)^2}\Big/\dfrac{5.6C_1^2\Gamma^2(\frac{2}{3})}{3\pi^2}\left(\dfrac{\delta_*}{L}\right)^{1/3}\left(\dfrac{U_c}{U}\right)^{7/3}\right\}$, (——) defined by Eq. (52) for conditions (53) when $M=0.1,\ \theta=30^\circ$. Also shown is the corresponding blocked pressure spectrum $10\times\log_{10}(\Phi_{pp}(U/\delta_*)/(\rho_0 v_*^2)^2)$ (- - - - , Eq. (50)) peaking at the second Rossiter mode $f\,L/U\sim 1$, and the cavity 'monopole' radiation (● ● ●).

The situation is very different at the higher Mach number $M=0.1$ (Fig. 4). The cavity mode resonance frequency $f\,L/U\sim 2.5$, and the monopole peak is several dB above the dipole peak at the Rossiter frequency ($f\,L/U=1$), although it should be observed that the magnitude of this peak scales approximately in proportion to $(\rho_0 U^2)^2M^2$, as for the dipole sound. The presence of this peak in the lower frequency region has a profound effect on the radiation directivity, as indicated in Fig. 5, in which the magnitude of

$$\frac{\Phi(\omega,\mathbf{x})(U/\delta_*)}{(\rho_0 v_*^2)^2(L/|\mathbf{x}|)^2}$$

is plotted against the radiation direction θ for $f\,L/U=0.5,\ 1,\ 1.5,\ 2,\ 2.5$, all curves being to the same scale. In Fig. 4 it can be seen that the lowest frequency $f\,L/U=0.5$ is sufficiently far from

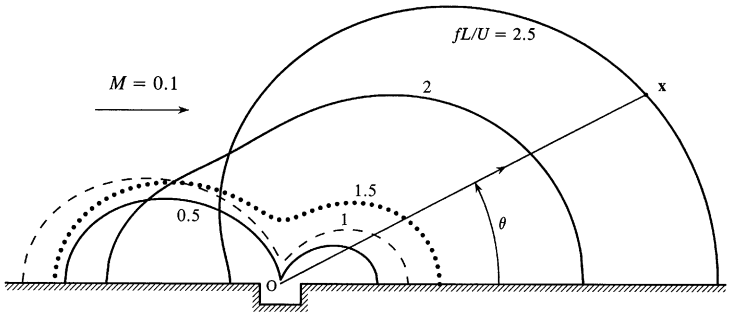

Fig. 5. Directivity $\dfrac{\Phi(\omega,\mathbf{x})(U/\delta_*)}{(\rho_0 v_*^2)^2(L/|\mathbf{x}|)^2}$ for a cavity of dimensions (53) for $M=0.1$ and $f\,L/U=0.5,\ 1,\ 1.5,\ 2,\ 2.5$ when the shear layer blocked pressure spectrum Φ_{pp} peaks at the second Rossiter mode $f\,L/U\sim 1$.

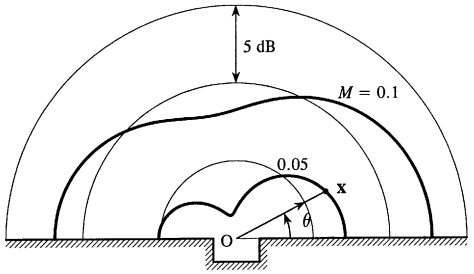

Fig. 6. Directivity $10\times\log_{10}(\langle p^2(\mathbf{x},t)\rangle/p_0^2)$ of overall sound radiated in the frequency range $0.1<f\,L/U<10$ for $M=0.05,\ 0.1$ for the cavity defined by Eq. (53).

the monopole peak to be effectively uninfluenced by the monopole. The directivity is therefore that of a dipole, peaking in the upstream and downstream directions, but subject to Doppler amplification by the mean flow, which causes the level to be larger in upstream directions. The dotted curves in Figs. 3 and 4 represent the field of the monopole cavity mode alone, when the term $\mathrm{i}(\cos\theta - M)$ on the right of Eq. (52) is deleted. This shows that the influence of the monopole is confined to the immediate vicinity of the resonance frequency. At higher frequencies the detailed directivity is determined by phase interference between the monopole and dipole, as well as the differences in the Doppler effects on both sources. Thus, at the spectral peak at $f\,L/U=2.5$ this interference produces strong radiation preferentially in the downstream direction.

An overall picture of the farfield radiation is obtained by integrating the spectrum (52) with respect to ω. The integral is convergent at $\omega=+\infty$, but contributions at very high frequencies are probably not representative. Therefore we depict in Fig. 6 for $M=0.05,\ 0.1$ the radiated pressure directivity when the integration is confined to the Strouhal number range $0.1<f\,L/U<10$. In both cases this includes the frequency range in which the monopole is important. At the lower Mach number the directivity resembles that of a dipole, but peaking in the downstream direction owing to modifications produced by the monopole resonant response. The situation at $M=0.1$ is similar except that there is significant radiation in directions normal to the wall.

5. Conclusion

At very low Mach numbers the aerodynamic sound generated by nominally steady flow over a shallow wall cavity is dominated by dipole radiation produced by the unsteady drag force, the radiation peaking in directions upstream and downstream of the cavity. The drag force fluctuations are produced by the interaction of vorticity, in an unstable mean shear layer or periodically ejected from the cavity, with the trailing edge of the cavity. It is the principal source in underwater applications where M rarely exceeds about 0.01, provided it is permissible to ignore structural resonances associated with hydrodynamic forcing of flexing cavity walls. In such cases the lowest, rigid body cavity resonance frequency (the 'Helmholtz' resonance frequency) tends to be large, and beyond the range where it can be effectively excited by the flow. At higher Mach numbers, however, the resonance frequency lies closer to the relevant 'Rossiter' modes of the unstable hydrodynamic flow over the cavity, and can then make a significant contribution to the radiation.

The cavity resonance produces a monopole contribution to the sound and is governed by compressible effects in the cavity region. At low Mach numbers these are usually very weak, such that whereas the intensity of the drag dipole exhibits the usual aeroacoustic dipole strength $\sim\rho_0 U^3 M^3$, the strength of the compressible-dominated, cavity source would vary as $\sim\rho_0 U^3 M^5$. However, when significant excitation of the cavity resonance occurs, say at Mach numbers exceeding about 0.05, the unsteady drag fluctuations also excite the cavity mode with a radiation intensity of the same order as the dipole sound. At these higher Mach numbers the radiation directivity at a frequency close to the cavity resonance is governed by the correlated interference between the dipole and monopole fields; at frequencies far removed from the resonance the directivity reverts to that of an isolated dipole. The overall sound power now tends to be uniformly distributed in direction; in particular there is significant radiation in the direction normal to the wall, which is otherwise a radiation null for the dipole alone.

The detailed results given in this paper are for a moderately shallow cavity dominated by shear layer mode instabilities, of the kind usually associated with the Rossiter modes. However, the Green's function developed in Section 3 can also be used to determine the cavity radiation for very shallow cavities, where an unsteady hydrodynamic 'wake flow' wets the cavity base, and the motion is characterized by the quasi-periodic ejection of cavity vorticity into the main flow. This ejection produces a violent fluctuation in the drag, which determines both the dipole and monopole sources of sound.

Acknowledgements

The work reported in this paper is supported by the Office of Naval Research under Grant N00014-02-1-0549 administered by Dr. L. Patrick Purtell. The author gratefully acknowledges the benefit of discussions with Dr. William K. Blake.

References

[1] J.E. Rossiter, The effect of cavities on the buffeting of aircraft, Royal Aircraft, Establishment Tech. Memo. 754, 1962.

[2] M.S. Howe, Edge, cavity and aperture tones at very low Mach numbers, *Journal of Fluid Mechanics* 330 (1997) 61–84.
[3] M.S. Howe, *Acoustics of Fluid-structure Interactions*, Cambridge University Press, Cambridge, 1998.
[4] D. Rockwell, Oscillations of impinging shear layers, *American Institute of Aeronautics and Astronautics Journal* 21 (1983) 645–664.
[5] N.M. Komerath, K.K. Ahuja, F.W. Chambers, Prediction and measurement of flows over cavities—a survey, American Institute of Aeronautics and Astronautics Paper 87-022, 1987.
[6] K.K. Ahuja, J. Mendoza, Effects of cavity dimensions, boundary layer, and temperature on cavity noise with emphasis on benchmark data to validate computational aeroacoustic codes, NASA Contractor Report 4653, Final Report Contract NAS1-19061, Task 13, 1995.
[7] D. Rockwell, E. Naudascher, Review—self-sustaining oscillation of flow past cavities, *Transactions of the American Society of Mechanical Engineers, Journal of Fluids Engineering* 100 (1978) 152–165.
[8] S.M. Grace, An overview of computational aeroacoustic techniques applied to cavity noise prediction, American Institute of Aeronautics and Astronautics Paper 2001-0510, 2001.
[9] M. Gharib, A. Roshko, The effect of flow oscillations on cavity drag, *Journal of Fluid Mechanics* 177 (1987) 501–530.
[10] T. Colonius, A. Basu, C. Rowley, Numerical investigation of flow past a cavity, American Institute of Aeronautics and Astronautics Paper 99-1912, 1999.
[11] D.F. Fuglsang, A.B. Cain, Evaluation of shear layer cavity resonances by numerical simulation, American Institute of Aeronautics and Astronautics Paper 92-0555, 1992.
[12] C.K.W. Tam, P.J.W. Block, On the tones and pressure oscillations induced by flow over rectangular cavities, *Journal of Fluid Mechanics* 89 (1978) 373–399.
[13] X. Zhang, Compressive cavity flow oscillations due to shear layer instabilities and pressure feedback, *American Institute of Aeronautics and Astronautics Journal* 33 (1995) 1404–1411.
[14] H.E. Plumblee, J.S. Gibson, L.W. Lassiter, A theoretical and experimental investigation of the acoustic response of cavities in an aerodynamic flow, US Air Force Report WADD-TR-61-75, 1962.
[15] L.F. East, Aerodynamically induced resonance in rectangular cavities, *Journal of Sound and Vibration* 3 (1966) 277–287.
[16] Y.H. Yu, Measurements of sound radiation from cavities at subsonic speeds, American Institute of Aeronautics and Astronautics Paper 76-529, 1976.
[17] M. Inagaki, O. Murata, T. Kondoh, Numerical prediction of fluid-resonant oscillation at low Mach number, *American Institute of Aeronautics and Astronautics Journal* 40 (2002) 1821–1829.
[18] M. Jacob, V. Gradoz, A. Louisot, S. Juve, S. Guerrand, Comparison of sound radiated by shallow cavities and backward facing steps. American Institute of Aeronautics and Astronautics Paper 99-1892, 1999.
[19] J.C. Hardin, D.S. Pope, An acoustic/viscous splitting technique for computational aeroacoustics, *Theoretical and Computational Aeroacoustics* 6 (1994) 323–340.
[20] J.C. Hardin, D.S. Pope, Sound generation by flow over a two-dimensional cavity, *American Institute of Aeronautics and Astronautics Journal* 33 (1995) 407–412.
[21] J.A. Ekaterinaris, New formulation of Hardin–Pope equations for aeroacoustics, *American Institute of Aeronautics and Astronautics Journal* 37 (1999) 1033–1039.
[22] W.Z. Shen, J.N. Sorensen, Comment on the aeroacoustic formulation of Hardin and Pope, *American Institute of Aeronautics and Astronautics Journal* 37 (1999) 141–143.
[23] S.M. Grace, C.K. Curtis, Acoustic computations using incompressible inviscid CFD results as input, *Proceedings of the ASME Noise Control and Acoustics Division NCA*, Vol. 26, ASME IMECE, Nashville, TN, November 1999.
[24] C. Curtis Granda, A Computational Acoustic Prediction Method Applied to Two-dimensional Cavity Flow, Master's Thesis, Boston University, December, 2001.
[25] G.K. Batchelor, *An Introduction to Fluid Dynamics*, Cambridge University Press, Cambridge, 1967.
[26] K. Taylor, A transformation of the acoustic equation with implications for wind tunnel and low speed flight tests, *Proceedings of the Royal Society of London* A363 (1978) 271–281.
[27] Lord Rayleigh, *Theory of Sound*, Vol. 2, Dover, New York, 1945.
[28] Horace Lamb, *Hydrodynamics*, 6th Edition, Cambridge University Press, Cambridge, 1932.

[29] C.K.W. Tam, The acoustic modes of a two-dimensional rectangular cavity, *Journal of Sound and Vibration* 49 (1976) 353–364.
[30] M.S. Howe, The influence of vortex shedding on the generation of sound by convected turbulence, *Journal of Fluid Mechanics* 76 (1976) 711–740.
[31] D.G. Crighton, The Kutta condition in unsteady flow, *Annual Reviews of Fluid Mechanics* 17 (1985) 411–445.
[32] T. Takaishi, A. Sagawa, K. Nagakura, T. Maeda, Numerical analysis of dipole sound source around high speed trains, *Journal of the Acoustical Society of America* 111 (2002) 2601–2608.
[33] M. Abramowitz, I.A. Stegun (Eds.), *Handbook of Mathematical Functions*, 9th Edition, National Bureau of Standards Applied Mathematics Series No. 55, US Department of Commerce, 1970.
[34] D.G. Crighton, Scattering and diffraction of sound by moving bodies, *Journal of Fluid Mechanics* 72 (1975) 209–227.